Gold(I) Heteroatom-Substituted Imido Complexes. Amino Nitrene Loss from $[(LAu)_3(\mu\text{-}NNR_2)]^+$

Bruce W. Flint, Yi Yang, and Paul R. Sharp*

Department of Chemistry, University of Missouri—Columbia, Columbia, Missouri 65211

Received May 20, 1999

The heteroatom-substituted imido complexes $[(LAu)_3(\mu\text{-}NX)]^+$ (X = NR_2, R = Ph, Me, Bz; X = OH, Cl; L = a phosphine) have been prepared from the reactions of NH_2X with $[(LAu)_3(\mu\text{-}O)]^+$. Thermally unstable $[(LAu)_3(\mu\text{-}NNMe_2)]^+$ (L = $P(p\text{-}XC_6H_4)_3$, X = H, F, Me, Cl, MeO) decompose to the gold cluster $[LAu]_6^{2+}$ and tetramethyltetrazene $Me_2NN{=}NNMe_2$. The decomposition is first-order overall with a rate constant that increases with increasing pK_a of the phosphine ligand. Activation parameters for the decomposition are $\Delta H^{\ddagger}$ = 99(4) kJ/mol and $\Delta S^{\ddagger}$ = 18.5(5) J/K·mol for L = PPh_3 and $\Delta H^{\ddagger}$ = 78(3) kJ/mol and $\Delta S^{\ddagger}$ = −47(2) J/K·mol for L = $P(p\text{-}MeOC_6H_4)_3$. The decomposition of analogous $[(LAu)_3(\mu\text{-}NNBz_2)]^+$ produces bibenzyl, indicative of the release of free amino nitrene Bz_2NN.

Introduction

Gold is exceptional in its ability to form compounds with unusual structures and properties. This chemistry features hypercoordinate complexes,[1] aurophilic attractions,[1−7] numerous clusters,[8−19] and recently a dinitrogen/hydrazido complex.[20] This dinitrogen/hydrazido complex $[(LAu)_6(\mu\text{-}N_2)]^{2+}$, formed from hydrazine, a common reducing agent, is remarkably stable despite the notorious susceptibility of Au ions to reduction. The gold(I) hydrazido complexes $[(LAu)_3(\mu\text{-}NNR_2)]^+$ are similarly produced from the substituted hydrazine R_2NNH_2.[9,21] Unlike the dinitrogen/hydrazido complex, $[(LAu)_3(\mu\text{-}NNR_2)]^+$ (R = alkyl) readily decompose in solution. Although Au is generally not catalytically active (see refs 22−27 for a growing number of exceptions), the stability of metal−nitrogen bonds is relevant to such diverse processes as ammonia oxidation,[28−30] NO_x and nitrite reduction,[31−33] and nitrogen fixation.[34] We have therefore undertaken a study of the decomposition of $[(LAu)_3(\mu\text{-}NNR_2)]^+$ and have examined the influence of the phosphine ligand's pK_a on the rate and activation parameters for the reaction. We have also prepared the related isoelectronic complexes $[(LAu)_3(\mu\text{-}NCl)]^+$ and $[(LAu)_3(\mu\text{-}NOH)]^+$ and briefly examined their stability.

Results

The white to yellow hydrazido complexes $[(LAu)_3(\mu\text{-}NNR_2)]^+$ (R = Ph, L = PPh_3;[21] R = CH_2Ph (Bz), L = PPh_3, $P(p\text{-}MeOC_6H_4)_3$; R = Me, L = PPh_3,[21] $PEtPh_2$, PPr^iPh_2, $P(o\text{-tol})_3$, $P(p\text{-}FC_6H_4)_3$, $P(p\text{-}ClC_6H_4)_3$, $P(p\text{-tol})_3$, $P(p\text{-}MeOC_6H_4)_3$) are

(1) Schmidbaur, H. *Chem. Soc. Rev.* **1995**, *24*, 391−400.
(2) Zank, J.; Schier, A.; Schmidbaur, H. *J. Chem. Soc., Dalton Trans.* **1998**, 323−324.
(3) Canales, F.; Gimeno, M. C.; Laguna, A.; Jones, P. G. *J. Am. Chem. Soc.* **1996**, *118*, 4839−4845.
(4) Harwell, D. E.; Mortimer, M. D.; Knobler, C. B.; Anet, F. A. L.; Hawthorne, M. F. *J. Am. Chem. Soc.* **1996**, *118*, 2679−2685.
(5) Pyykkö, P.; Runeberg, N.; Mendizabal, F. *Chem. Eur. J.* **1997**, *3*, 1451−1457.
(6) Veiros, L. F.; Calhorda, M. J. *J. Organomet. Chem.* **1996**, *510*, 71−81.
(7) Grandberg, K. I.; Dyadchenko, V. P. *J. Organomet. Chem.* **1994**, *474*, 1−21.
(8) Yang, Y.; Sharp, P. R. *J. Am. Chem. Soc.* **1994**, *116*, 6983−6984.
(9) Yang, Y.; Wu, Z.; Ramamoorthy, V.; Sharp, P. R. *The Chemistry of the Copper and Zinc Triads*; Welch, A. J., Chapman, S. K., Eds.; The Royal Society of Chemistry: Cambridge, 1993.
(10) Mingos, D. M. P.; Watson, M. J. *Adv. Inorg. Chem.* **1996**, *39*, 327−399.
(11) Hall, K. P.; Mingos, D. M. P. *Prog. Inorg. Chem.* **1984**, *32*, 237−325.
(12) Laguna, A.; Laguna, M.; Gimeno, M. C.; Jones, P. G. *Organometallics* **1992**, *11*, 2759−2760.
(13) Copley, R. C. B.; Mingos, D. M. P. *J. Chem. Soc., Dalton Trans.* **1996**, 479−489.
(14) Copley, R. C. B.; Mingos, D. M. P. *J. Chem. Soc., Dalton Trans.* **1996**, 491−500.
(15) Shan, H.; Sharp, P. R. *Angew. Chem., Int. Ed. Engl.* **1996**, *35*, 635−636.
(16) Crespo, O.; Gimeno, M. C.; Jones, P. G.; Laguna, A.; Villacampa, M. D. *Angew. Chem., Int. Ed. Engl.* **1997**, *36*, 993−995.
(17) Schmid, G. *Chem. Rev.* **1992**, *92*, 1709.
(18) Teo, B. K.; Dang, H.; Campana, C. F.; Zhang, H. *Polyhedron* **1998**, *17*, 617−621.
(19) Teo, B. K.; Zhang, H.; Shi, X. *Inorg. Chem.* **1994**, *33*, 4086−4097.
(20) Shan, H.; Yang, Y.; James, A. J.; Sharp, P. R. *Science* **1997**, *275*, 1460−1462.
(21) Ramamoorthy, V.; Wu, Z.; Yang, Y.; Sharp, P. R. *J. Am. Chem. Soc.* **1992**, *114*, 1526−1527.
(22) Haruta, M.; Tsubota, S.; Kobayashi, T.; Kageyama, H.; Genet, M. J.; Delmon, B. *J. Catal.* **1993**, *144*, 175−192.
(23) Hoflund, G. B.; Gardner, S. D.; Schryer, D. R.; Upchurch, B. T.; Kielin, E. J. *Appl. Catal., B* **1995**, *6*, 117−126.
(24) Sakurai, H.; Haruta, M. *Appl. Catal. A* **1995**, *127*, 93−105.
(25) Sakurai, H.; Ueda, A.; Kobayashi, T.; Haruta, M. *J. Chem. Soc., Chem. Commun.* **1997**, 271−272.
(26) Valden, M.; Lai, X.; Goodman, D. W. *Science* **1998**, *281*, 1647−1650.
(27) Ueda, A.; Oshima, T.; Haruta, M. *Appl. Catal., B* **1997**, *12*, 81−93.
(28) Ishitani, O.; White, P. S.; Meyer, T. J. *Inorg. Chem.* **1996**, *35*, 2167−2168.
(29) Carley, A. F.; Davies, P. R.; Roberts, M. W. *Chem. Commun.* **1998**, 1793−1794.
(30) Trombetta, M.; Ramis, G.; Busca, G.; Montanari, B.; Vaccari, A. *Langmuir* **1997**, *13*, 4628−4637.
(31) Murphy, W. R. Jr.; Takeuchi, K.; Barley, M. H.; Meyer, T. J. *Inorg. Chem.* **1986**, *25*, 1041−1053.
(32) Burch, R.; Fornasiero, P.; Southward, B. W. L. *Chem. Commun.* **1998**, 739−740.
(33) Connerton, J.; Joyner, R. W.; Stockenhuber, M. *Chem. Commun.* **1997**, 185−186.
(34) Hidai, M.; Mizobe, Y. *Chem. Rev.* **1995**, *95*, 1115.

10.1021/ic990586u CCC: $19.00
Published on Web 01/21/2000

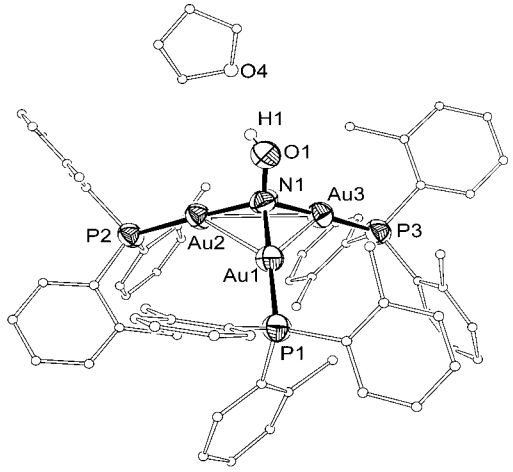

Figure 1. ORTEP drawing of the cationic portion of $[\{(o\text{-tol})_3PAu\}_3(\mu\text{-NOH})]BF_4$ with a hydrogen-bonded THF molecule.

obtained from $[(LAu)_3(\mu\text{-O})]^+$ and the 1,1-substituted hydrazines R_2NNH_2 according to eq 1. Several of these complexes are very unstable in solution and must be isolated quickly to avoid decomposition (see below). Once isolated in the solid state, the complexes are stable.

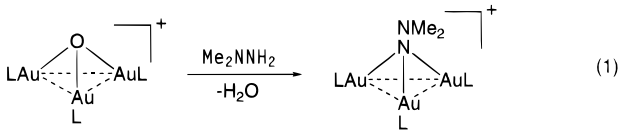

(1)

An attempt was also made to prepare $[(Ph_3PAu)_3(\mu\text{-NNPr}^i_2)]^+$ according to eq 1 ($R = Pr^i$). A reaction between the oxo complex and $Pr^i_2NNH_2$ does occur, but the hydrazido complex is not detected. Instead, the gold cluster[11] $[(Ph_3PAu)_6]^{2+}$ and $Pr^i_2NN{=}NNPr^i_2$ form as the oxo complex $[(Ph_3PAu)_3(\mu\text{-O})]^+$ is consumed. These are the same types of products produced in the decomposition of $[(Ph_3PAu)_3(\mu\text{-NNMe}_2)]^+$ (see below), suggesting that $[(Ph_3PAu)_3(\mu\text{-NNPr}^i_2)]^+$ is formed but decomposes as quickly as it is produced.

Two other gold heteroatom-substituted imido complexes are prepared in reactions similar to that shown in eq 1. Colorless $[(LAu)_3(\mu\text{-NOH})]^+$ is formed by treating $[(LAu)_3(\mu\text{-O})]^+$ with hydroxylamine NH_2OH (eq 2, X = OH, L = PPh_3, P(*o*-tol)$_3$),

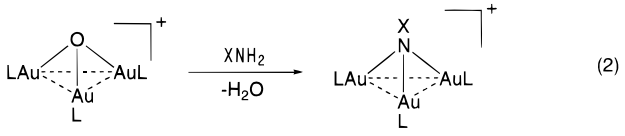

(2)

and $[(LAu)_3(\mu\text{-NCl})]^+$ is the product from the reaction of $[(LAu)_3(\mu\text{-O})]^+$ with chloramine NH_2Cl (eq 2, X = Cl, L = PPh_3). The triphenylphosphine derivative $[(Ph_3PAu)_3(\mu\text{-NOH})]^+$ is too unstable to isolate in pure form and decomposes cleanly to the cluster $[(Ph_3PAu)_6]^{2+}$. In contrast, the (*o*-tol)$_3$P derivative $[\{(o\text{-tol})_3PAu\}_3(\mu\text{-NOH})]^+$ is stable in solution. $[(Ph_3PAu)_3(\mu\text{-NCl})]^+$ decomposes over several hours at ambient temperatures to mixtures of Ph_3PAuCl and the nitrido complex $[(Ph_3PAu)_5N]^+$.[1] The nitrido complex is also a major decomposition product of the silyl imido complexes $[(LAu)_3(\mu\text{-NSiR}_3)]^+$.[35]

An X-ray crystal structure determination of $[((o\text{-tol})_3PAu)_3(\mu\text{-NOH})](BF_4)$ confirms the expected structure. A drawing of the cationic portion is given in Figure 1 and includes a THF molecule hydrogen-bonded to the hydrogen atom of the NOH group. An abbreviated summary of crystal data collection and processing is given in Table 1. Selected bond distances and angles are listed in Table 2. The structure of the complex closely resembles those of the many other $[(LAu)_3(\mu\text{-E})]^+$ derivatives[7,21,35−43] including related $[(LAu)_3(\mu\text{-NOSiMe}_3)]^+$.[44]

Table 1. Crystallographic and Data Collection Parameters for $[\{(o\text{-tol})_3PAu\}_3(\mu\text{-NOH})]BF_4\cdot 3THF$ and $[(Ph_3PAu)_3(\mu\text{-NNMe}_2Et)](OTf)_2\cdot 3THF$

empirical formula	$C_{75}H_{88}Au_3BF_4NO_4P_3$	$C_{72}H_{80}Au_3F_6N_2O_9P_3S_2$
fw	1838.17	1979.31
space group	$P2_1/n$ (no. 14)	$P\bar{1}$ (no. 2)
T (°C)	298	173
a (Å)	15.813(8)	12.9750(8)
b (Å)	26.145(4)	14.5771(9)
c (Å)	17.768(8)	22.0437(14)
α (deg)		71.750(1)
β (deg)	96.98(2)	89.420(1)
γ (deg)		68.236(1)
V (Å^3)	7291(5)	3650.7(4)
Z	4	2
d_{calcd} (g/cm^3)	1.67	1.80
λ (Å)	0.7093 (Mo)	0.7093 (Mo)
μ (mm^{-1})	6.14	6.21
R1,[a] wR2[b]	0.0499, 0.1320	0.0513, 0.1079

[a] $R1 = (\sum||F_o| - |F_c||)/\sum|F_o|$. [b] $wR2 = [(\sum w(F_o^2 - F_c^2)^2)/\sum w(F_c^2)^2]^{1/2}$ with $w = 1/[\sigma^2(F_o^2) + (xP)^2]$; $P = (F_o^2 + 2F_c^2)/3$, $x =$ 0.1025 (NOH complex) and 0.0649 ($NNMe_2Et$ complex).

The decomposition of the hydrazido complex $[(LAu)_3(\mu\text{-NNMe}_2)]^+$ (L = PPh_3) has been reported to follow eq 3.[21]

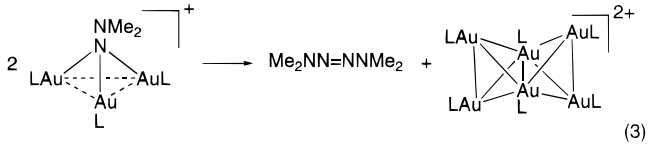

(3)

Consistent with previous work showing that the nuclearity of phosphine gold clusters is dependent on the cone angle of the phosphine ligand,[11] this same equation also describes the decomposition of the dimethylhydrazido $[(LAu)_3(\mu\text{-NNMe}_2)]^+$ complexes with L = a para-substituted arylphosphine ligand (cone angle 145°, same as for PPh_3) or PPh_2Pr^i (cone angle 150°). The product edge-shared bitetrahedral gold clusters $[(LAu)_6]^{2+}$ are readily identified by their known fluxional behavior and characteristic UV−vis spectra.[11] The fluxional process involves exchange of the edge-shared positions with the wing-tip positions and is observed in both proton and ^{31}P NMR spectra. Ambient-temperature ^{31}P NMR spectra of the para-substituted aryl phosphine ligand clusters show similar shifts and fast exchange (single sharp peak) while the PPh_2Pr^i cluster shows intermediate exchange (very broad peak). Low-temperature spectra show the expected pair of peaks in a 2:1

(35) Angermaier, K.; Schmidbaur, H. *Chem. Ber.* **1995**, *128*, 817−822.
(36) Nesmeyanov, A. N.; Perevalova, E. G.; Struchkov, Y. T.; Antipin, M. Y.; Grandberg, K. I.; Dyadchenko, V. P. *J. Organomet. Chem.* **1980**, *201*, 343−349.
(37) Ramamoorthy, V.; Sharp, P. R. *Inorg. Chem.* **1990**, *29*, 3336−3338.
(38) Yang, Y.; Sharp, P. R. *Inorg. Chem.* **1993**, *32*, 1946−1951.
(39) Angermaier, K.; Schmidbaur, H. *J. Chem. Soc., Dalton Trans.* **1995**, 559−564.
(40) Kolb, A.; Bissinger, P.; Schmidbaur, H. *Z. Anorg. Allg. Chem.* **1993**, *619*, 1580−1588.
(41) Canales, F.; Gimeno, M. C.; Jones, P. G.; Laguna, A. *Angew. Chem., Int. Ed. Engl.* **1994**, *33*, 769−770.
(42) Vincente, J.; Chicote, M.-T.; Guerrero, R.; Jones, P. G.; de Arellano, M. C. R. *Inorg. Chem.* **1997**, *36*, 4438−4443.
(43) Kuz'mina, L. G. *Zh. Neorg. Khim.* **1993**, *38*, 994−1003.
(44) Tripathi, U. M.; Scherer, W.; Schier, A.; Schmidbaur, H. *Inorg. Chem.* **1998**, *37*, 174−175.

Table 2. Selected Distances (Å) and Angles (deg) for $[(LAu)_3(\mu\text{-NOH})]BF_4$ (L = P(*o*-tol)$_3$)

Au1−Au3	3.1412 (7)	Au1−Au2	3.1946 (7)	Au2−Au3	3.1767 (7)
Au1−P1	2.249 (4)	Au2−P2	2.251 (3)	Au3−P3	2.248 (4)
Au1−N1	2.041 (10)	Au2−N1	2.033 (10)	Au3−N1	2.000 (10)
O1−N1	1.421 (13)				
Au3−N1−Au2	103.9 (5)	Au3−N1−Au1	102.0 (4)		
Au2−N1−Au1	103.3 (5)	N1−Au1−P1	177.2 (3)		
N1−Au2−P2	177.7 (3)	N1−Au3−P3	177.4 (3)		
N1−Au3−Au1	39.5 (3)	O1−N1−Au3	116.5 (8)		
O1−N1−Au2	116.4 (7)	O1−N1−Au1	112.8 (8)		

Table 3. Phosphine pK_a Values and Rate Constant Data for Decomposition of $[(LAu)_3(\mu\text{-NNMe}_2)]BF_4$ at 298 K

L	pK_a[a]	k (s^{-1}) × 10^3	L	pK_a[a]	k (s^{-1}) × 10^3
(*p*-ClC_6H_4)$_3$P	1.03	0.63(2)	(*p*-tol)$_3$P	3.84	0.22(1)
(*p*-FC_6H_4)$_3$P	1.97	0.43(2)	(*p*-$MeOC_6H_4$)$_3$P	4.59	0.28(1)
Ph_3P	2.73	0.30(1)			

[a] pK_a data taken from ref 45.

ratio. Evidently, exchange is more rapid for the clusters with the smaller cone angle para-substituted arylphosphine ligands than for the cluster with the slightly larger cone angle phosphine PPh_2Pr^i.

The known[11] larger cluster $[(LAu)_{10}Au]^{3+}$ and $[L_2Au]^+$ are the gold-containing products with the smaller cone angle phosphine ligands L = PMe_2Ph (cone angle 122°) and PPh_2-Me (cone angle 136°, eq 4). Again, this is consistent with previous work showing that the main determinant of the nuclearity of phosphine gold clusters is the cone angle of the phosphine ligand.[11]

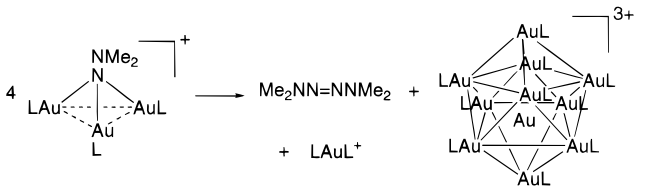

(4)

In an earlier communication the kinetics for the reaction in eq 3 for L = PPh_3 were reported to be second order.[21] Subsequent reaction studies cast doubt on this result, and a re-evaluation of the previous experiments revealed a systematic error in the measurements that incorrectly led to this assignment. Kinetic measurements have been repeated here for the PPh_3 complex and completed for several para-substituted arylphosphine ligand complexes. The decomposition of eq 3 is first order in all cases studied.

First-order plots are given as Supporting Information. Rate constants and pK_a values for the phosphine ligands (taken from ref 45) are listed in Table 3, and a plot of log *k* versus the pK_a of the phosphine ligand is shown in Figure 2. A similar plot (Supporting Information) but with an opposite slope is obtained when log *k* is plotted against the phosphine ligand electronic parameter χ.[46,47] An inverse relationship between the pK_a and χ values of the phosphine ligand is expected with this set of isosteric, σ-donor ligands.[48−50] With the exception of L = P(*p*-$MeOC_6H_4$)$_3$, a linear relationship ($r^2 = 0.988$) is observed with larger pK_a values, giving smaller *k* values. A larger pK_a value

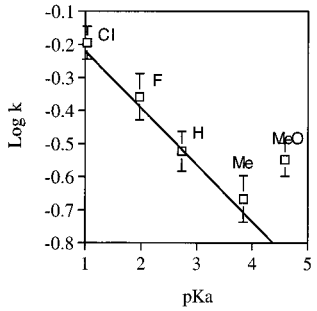

Figure 2. log of the rate constants (298 K) for the decomposition of $[(LAu)_3(\mu\text{-NNMe}_2)]BF_4$ versus the pK_a of L. The line represents the least-squares fit excluding L = (*p*-$MeOC_6H_4$)$_3$P.

indicates a stronger donor ligand, which retards the decomposition and gives a more stable hydrazido complex.

The temperature dependence of the rate constant was evaluated for L = PPh_3 and P(*p*-$MeOC_6H_4$)$_3$. Data and a plot of ln *k* versus 1/*T* are given in the Supporting Information. Extracted activation parameters are $\Delta H^{\ddagger} = 99(4)$ kJ/mol and $\Delta S^{\ddagger} = 18.5(5)$ J/K·mol for L = PPh_3 and $\Delta H^{\ddagger} = 78(3)$ kJ/mol and $\Delta S^{\ddagger} = -47(2)$ J/K·mol for L = P(*p*-$MeOC_6H_4$)$_3$.

The first-order decomposition of the hydrazido complexes and the formation of tetramethyltetrazene suggest the formation and dimerization of the nitrene Me_2NN. FAB mass spectral data for $[(LAu)_3(\mu\text{-NNMe}_2)]^+$ (L = PPh_3) are also suggestive of nitrene loss and show the $[(LAu)_3]^+$ cluster as the major mass peak above 1000. Experiments designed to trap free nitrene in the decomposition were unsuccessful probably due to the low reactivity of amino nitrenes.[51] As an alternative approach, the hydrazido complexes $[(LAu)_3(\mu\text{-NNBz}_2)]^+$ (L = PPh_3, P(*p*-$MeOC_6H_4$)$_3$) were prepared as described above, and their decompositions were examined. These compounds are more stable than the dimethyl analogues and decompose over several days to bibenzyl and $[(LAu)_6]^{2+}$ (eq 5). Tetrabenzyltetrazene is not detected. The formation of bibenzyl is indicative of free Bz_2NN, where the stability of the benzyl radical permits decomposition of the nitrene to bibenzyl and dinitrogen before dimerization.[51]

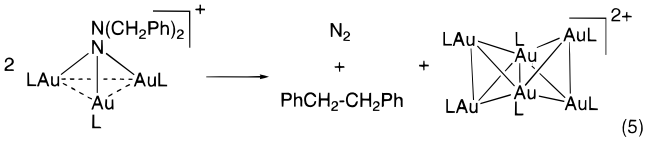

(5)

The likely involvement of the hydrazido nitrogen lone pair in the decomposition of $[(LAu)_3(\mu\text{-NNR}_2)]^+$ prompted us to investigate the reaction of $[(LAu)_3(\mu\text{-NNR}_2)]^+$ with alkylating

(45) Rahman, Md. M.; Liu, H. Y.; Prock, A.; Giering, W. P. *Organometallics* **1987**, *6*, 650−658.
(46) Tolman, C. A. *Chem. Rev.* **1977**, *77*, 313−348.
(47) Bartik, T.; Himmler, T.; Schulte, H.; Seevogel, K. J. *J. Organomet. Chem.* **1984**, *272*, 29.
(48) Liu, H.-Y.; Eriks, K.; Prock, A.; Giering, W. P. *Organometallics* **1990**, *9*, 1758−1766.
(49) Rahman, Md. M.; Liu, H. Y.; Prock, A.; Giering, W. P. *Organometallics* **1989**, *8*, 1−7.
(50) Hudson, R. H. E.; Poë, A. J. *Organometallics* **1995**, *14*, 3238−3248.
(51) Loffe, B. V. *Russ. Chem. Rev.* **1972**, *41*, 131.

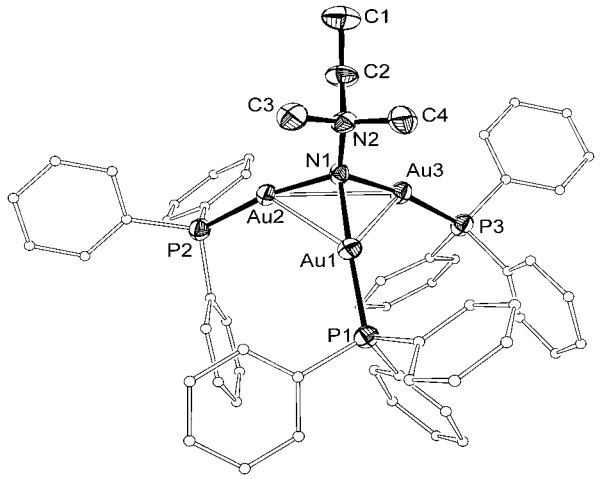

Figure 3. ORTEP drawing of the cationic portion of $[(Ph_3PAu)_3(\mu\text{-}NNMe_2Et)](OTf)_2$.

reagents. Addition of methyl or ethyl triflate to a decomposing solution of $[(Ph_3PAu)_3(\mu\text{-}NNMe_2)]^+$ results in a stable solution of $[(Ph_3PAu)_3(\mu\text{-}NNRMe_2)]^{2+}$ (R = Me, Et, eq 6). The alkylated complexes are much more stable than the parent hydrazido complexes and solutions remain unchanged for days. Related $[(LAu)_3(\mu\text{-}NPR_3)]^{2+}$ are also known to be very stable.[52,53]

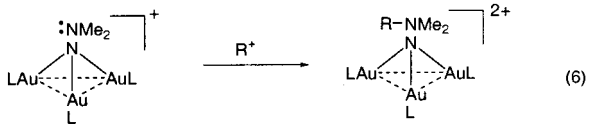

(6)

An X-ray crystal structure determination of $[(Ph_3PAu)_3(\mu\text{-}NNEtMe_2)](OTf)_2$ confirms the expected structure. A drawing of the cationic portion is given in Figure 3. An abbreviated summary of crystal data collection and processing is given in Table 1. Selected bond distances and angles are listed in Table 4. As with the hydroxylamine complex, the structure closely resembles those of the many other $[(LAu)_3(\mu\text{-}E)]^+$ derivatives.[7,21,35−44]

Discussion

A proposed mechanism for the decomposition of $[(LAu)_3(\mu\text{-}NNR_2)]^+$, consistent with the evidence of free nitrene, mass spectral data, and the first-order reaction rate, is given in Scheme 1. The rate-determining step involves the release of the stabilized amino nitrene NNR_2 (see resonance forms) from the three gold centers of $[(LAu)_3(\mu\text{-}NNR_2)]^+$. The amino nitrene NNR_2 may than follow two paths (A and B). A review of the chemistry of *N*-nitrenes by Loffe[51] discusses various studies of substituted hydrazine oxidation and the fate of the resulting amino nitrenes. Amino nitrenes containing R groups with relatively stable radicals (such as benzyl, allyl, and nitrile groups) favor decomposition to R_2 and N_2, while those containing R groups with less stable radicals (such as Me and Pr^i) survive long enough to dimerize to the tetrazene (Scheme 1, path A). The observation of tetrazine for R = Me and Pr^i and bibenzyl for R = Bz in the decomposition of $[(LAu)_3(\mu\text{-}NNR_2)]^+$ is indicative of the formation of free amino nitrenes.

The rate-determining step in Scheme 1 involves the formal reduction of two of the three Au(I) centers of the hydrazido complex to Au(0). The general trend of greater stability of $[(LAu)_3(\mu\text{-}NNR_2)]^+$ with more strongly donating L is consistent with this process, where greater donation from L stabilizes the Au(I) centers to reduction. The deviation of the L = P(*p*-$MeOC_6H_4)_3$ derivative is unusual. Linear relationships between the log of reaction rate constants and phosphine ligand pK_a values (or the phosphine ligand electronic parameter, χ) have been found for other systems, and para-substituted triarylphosphines have generally fallen on the linear line.[54] The deviation of the L = P(*p*-$MeOC_6H_4)_3$ derivative is discussed below in conjunction with the activation parameters.

The qualitatively decreasing stability of the complexes $[(Ph_3PAu)_3(\mu\text{-}NNR_2)]^+$, R = Ph > Bz > Me > Pr^i, is also consistent with reduction of the gold(I) centers in the rate-determining step and follows the expected increasing reducing strength of the hydrazido unit. Steric factors in this sequence are unlikely to be significant as the R groups are fairly far removed from the Au centers. This is supported by an examination of the structure of $[(Ph_3PAu)_3(\mu\text{-}NNMe_2Et)]^{2+}$, which does not show any close intracation contacts involving the $NNMe_2Et$ group.

Although the comparison is less direct, $[(Ph_3PAu)_3(\mu\text{-}NOH)]^+$ is much less stable than its closest analogue $[(Ph_3PAu)_3(\mu\text{-}NNMe_2)]^+$ and decomposes to give reduced Au centers. This suggests that the HON group is more strongly reducing than the R_2NN group, which is inconsistent with the expected greater donor strength of R_2N over HO. However, we do not know the decomposition mechanism of the hydroxylamine complex, where factors such as hydrogen bonding (see Figure 1) may be involved. The Me_3SiON complex is apparently stable,[44] but the Me_3Si group is electron withdrawing, and the Me_3SiON group is expected to be less reducing than the HON group. Investigation of the *O*-methylhydroxylamine complex would be informative.

Further support for amino nitrene loss is the positive $\Delta S^{\ddagger}$ for the decomposition of $[(Ph_3PAu)_3(\mu\text{-}NNMe_2)]^+$. Positive values for $\Delta S^{\ddagger}$ are indicative of "loose" or simple fission transition states[55] such as that expected in the rupture of the Au−N bonds. The relatively large negative value of $\Delta S^{\ddagger}$ for the L = P(*p*-$MeOC_6H_4)_3$ derivative is in sharp contrast and suggests a more ordered transition state. The $\Delta H^{\ddagger}$ values also differ significantly. Consistent with the unexpectedly facile decomposition of the L = P(*p*-$MeOC_6H_4)_3$ derivative, the transition state for the L = P(*p*-$MeOC_6H_4)_3$ derivative is 20 kJ/mol more accessible than that for the L = PPh_3 derivative. These differences do not affect the products of the decomposition, and evidence for free nitrene (formation of bibenzyl) is found for both phosphine ligand derivatives.

The results for the P(*p*-$MeOC_6H_4)_3$ derivative suggest that the complex is able to achieve a configuration or conformation where the Au(I) centers are more easily reduced than expected from the pK_a value of P(*p*-$MeOC_6H_4)_3$. This in turn suggests that the phosphine ligand can transiently become a weaker donor. The *p*-MeO group is unique in the series studied here in that the effect of this para-substituent primarily involves resonance donation into the phenyl ring (Scheme 2). (In fact, the weaker inductive effect of the MeO substituent is opposite and withdraws electron density from the ring.) Maximum resonance donation requires that the MeO group lie in the plane of the phenyl ring. Rotation of the MeO group out of optimum donation reduces the phosphine donor strength. This process,

(52) Bauer, A.; Gabbai, F.; Schier, A.; Schmidbaur, H. *Philos. Trans. R. Soc. London, Ser. A* **1996**, *354*, 381−394.
(53) Bauer, A.; Mitzel, N. W.; Schier, A.; Rankin, D. W. H.; Schmidbaur, H. *Chem. Ber.* **1997**, *130*, 323.
(54) Golovin, M. N.; Rahman, M. M.; Belmonte, J. E.; Giering, W. P. *Organometallics* **1985**, *4*, 1981−1991.
(55) Gilbert, R. *Theory of Unimolecular Recombination Reactions*; Blackwell Scientific: Oxford, England, 1990.

Table 4. Selected Distances (Å) and Angles (deg) for $[(Ph_3PAu)_3(\mu\text{-}NNMe_2Et)](OTf)_2$

Au1−Au3	2.9813 (5)	Au1−Au2	3.0669 (5)	Au2−Au3	3.1626 (5)
Au1−P1	2.246 (2)	Au2−P2	2.239 (2)	Au3−P3	2.241 (2)
Au1−N1	2.082 (6)	Au2−N1	2.052 (7)	Au3−N1	2.084 (6)
N1−N2	1.456 (9)				
Au2−N1−Au1	95.8 (3)	Au2−N1−Au3	99.8 (3)		
Au1−N1−Au3	91.4 (2)	N1−Au1−P1	171.93 (18)		
N1−Au2−P2	169.76 (18)	N1−Au3−P3	170.69 (19)		
N2−N1−Au1	121.1 (5)	N2−N1−Au2	122.3 (5)		
N2− N1−Au3	119.8(5)				

Scheme 1

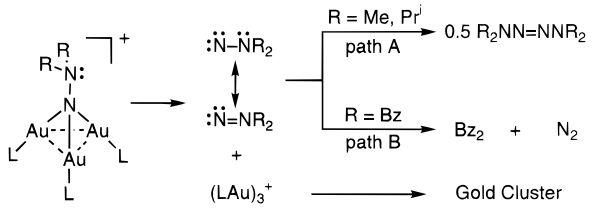

Scheme 2

occurring on one or more of the rings of the phosphine ligands, would lead to an easier than expected reduction of the Au(I) centers and, as a more organized configuration, a negative $\Delta S^{\ddagger}$. As a transient kinetic effect this would not contribute significantly to pK_a and other thermodynamic measurements.[56−60] It may not have been observed in other kinetic studies[50,61−74] either because the reactions are relatively insensitive to electronic contribution or because reaction acceleration occurs with increasing phosphine ligand donor strength (e.g., oxidative addition and nucleophilic attack by phosphines), opposite that with the hydrazido complexes here.

Somewhat surprisingly, considering the low coordination number of gold(I), phosphine ligand steric factors appear to be important in the stability of these complexes. This is shown most clearly by the qualitatively greater stability of the L = $(o\text{-tol})_3$P over the L = $(p\text{-tol})_3$P derivatives despite a lower pK_a value for $(o\text{-tol})_3$P (3.08 versus 3.84). We have previously noted a phosphine ligand steric effect in the structures of the oxo complexes $[(LAu)_3(\mu\text{-}O)]^+$, where the Au_3O tetrahedron expands at the Au_3 base with an increase in the phosphine ligand's cone angle.[38] This results in longer Au−Au distances, which could be an important parameter here as the release of the nitrene is expected to be accompanied by the formation of cluster Au−Au bonds. This implies that the "aurophilic" interaction[1−7] is a vital component in the decomposition reaction.

Finally, we come to the question of why the hydrazido complexes $[(LAu)_3(\mu\text{-}NNR_2)]^+$ are less stable than the dinitrogen complex $[(LAu)_3(\mu\text{-}N_2)(AuL)_3]^{2+}$. Given the decomposition mechanism of Scheme 1, it is apparent that the stabilization of the nitrene by the lone pair on the amino group is critical. Such a lone pair is absent in the dinitrogen complexes. Elimination of the nitrogen lone pair of $[(LAu)_3(\mu\text{-}NNMe_2)]^+$ by alkylation does effectively halt decomposition in the product $[(LAu)_3(\mu\text{-}NNRMe_2)]^{2+}$ (R = Me, Et).

Conclusions

We have reported the synthesis and characterization of a series of heteroatom-substituted gold imido complexes including the novel complex $[(LAu)_3(\mu\text{-}NCl)]^+$. We have demonstrated that, with the exception of L = $P(p\text{-}MeOC_6H_4)_3$, the stability of the $[(LAu)_3(\mu\text{-}NNR_2)]^+$ has a linear free energy relationship with the donor strength (pK_a) of the phosphine ligand L. The decomposition of $[(LAu)_3(\mu\text{-}NNR_2)]^+$ involves the release of a free nitrene NNR_2 with, for L = PPh_3, a "loose" transition state. A more ordered transition state and a faster than expected decomposition rate for L = $P(p\text{-}MeOC_6H_4)_3$ are attributed to resonance donation loss in the phosphine ligand by rotation of the MeO group out of the phenyl ring plane. Decomposition is blocked by alkylation of the hydrazido ligand, thereby eliminating the stabilizing nitrogen lone pair. Larger phosphine ligands retard the decomposition, suggesting that Au−Au interactions are also important in the transition state.

Experimental Section

General Procedures. Unless otherwise stated, the reactions were performed under a nitrogen atmosphere using a VAC drybox or Schlenk techniques. Dry THF, toluene, diethyl ether, CH_2Cl_2, and hexane were obtained by passing the solvent down an activated alumina column. Non-chlorine-containing solvents were stored over Na shavings. Me_2NNH_2 and Ph_2NNH_2·HCl were purchased from Aldrich Chemical Co. and used as received. $[(LAu)_3(\mu\text{-}O)]X$ (X = BF_4, OTf),[36,38,40] 1,1-dibenzylhydrazine,[75] 1,1-diisopropylhydrazine,[76] hydroxylamine,[77] and chloroamine[78] were prepared according to literature procedures. Infrared

(56) Li, C.; Nolan, S. P. *Organometallics* **1995**, *14*, 1327−1332.
(57) Serron, S. A.; Luo, L. B.; Li, C. B.; Cucullu, M. E.; Stevens, E. D.; Nolan, S. P. *Organometallics* **1995**, *14*, 5290−5297.
(58) Serron, S. A.; Nolan, S. P. *Organometallics* **1995**, *14*, 4611−4616.
(59) Serron, S.; Nolan, S. P.; Moloy, K. G. *Organometallics* **1996**, *15*, 4301−4306.
(60) Haar, C. M.; Nolan, S. P.; Marshall, W. J.; Moloy, K. G.; Prock, A.; Giering, W. P. *Organometallics* **1999**, *18*, 474−479.
(61) Chalk, K. L.; Pomeroy, R. K. *Inorg. Chem.* **1984**, *23*, 444−449.
(62) Chen, L.; Poë, A. J. *Inorg. Chem.* **1989**, *28*, 3641−3647.
(63) Wilson, M. R.; Woska, D. C.; Prock, A.; Giering, W. P. *Organometallics* **1993**, *12*, 1742−1752.
(64) Wilson, M. R.; Liu, H.; Prock, A.; Giering, W. P. *Organometallics* **1993**, *12*, 2044.
(65) Bartholomew, J.; Fernandez, A. L.; Lorsbach, B. A.; Wilson, M. R.; Prock, A.; Giering, W. P. *Organometallics* **1996**, *15*, 295−301.
(66) Fernandez, A.; Reyes, C.; Wilson, M. R.; Woska, D. C.; Prock, A.; Giering, W. P. *Organometallics* **1997**, *16*, 342−348.
(67) Fernandez, A.; Reyes, C.; Prock, A.; Giering, W. P. *Organometallics* **1998**, *17*, 2503−2509.
(68) Neubrand, A.; Poë, A. J.; Vaneldik, R. *Organometallics* **1995**, *14*, 3249−3258.
(69) Chen, L. Z.; Poë, A. J. *Coord. Chem. Rev.* **1995**, *143*, 265−295.
(70) Farrar, D. H.; Hao, J. B.; Poë, A. J.; Stromnova, T. A. *Organometallics* **1997**, *16*, 2827−2832.
(71) Romeo, R.; Plutino, M. R.; Scolaro, L. M.; Stoccoro, S. *Inorg. Chim. Acta* **1997**, *265*, 225−233.
(72) Romeo, R.; Alibrandi, G. *Inorg. Chem.* **1997**, *36*, 4822−4830.
(73) Bessel, C. A.; Margarucci, J. A.; Acquaye, J. H.; Rubino, R. S.; Crandall, J.; Jircitano, A. J.; Takeuchi, K. J. *Inorg. Chem.* **1993**, *32*, 5779.
(74) Moreno, C.; Delgado, S.; Macazaga, J. M. *Organometallics* **1991**, *10*, 1124.
(75) Dewar, M. J. S. *J. Am. Chem. Soc.* **1973**, *95*, 1562.
(76) Lemal, D. M.; Menger, F.; Coats, E. *J. Am. Chem. Soc.* **1964**, *86*, 2395.
(77) Hurd, C. D. *Inorg. Synth.* **1973**, *1*, 87−89.
(78) Coleman G. H.; Johnson, H. L. *Inorg. Synth.* **1973**, *1*, 59−62.

spectra were obtained with a Nicolet Magna-550 spectrometer. UV−vis absorption spectra were recorded on a Hewlett-Packard 8452A diode-array spectrophotometer. NMR spectra were recorded on a Bruker ARX-250 NMR or a Bruker AMX-500 instrument at ambient temperature unless otherwise indicated. ^{1}H and ^{31}P chemical shifts are reported in parts per million and are referenced to TMS (internal) and 85% H_3PO_4 (external) standards, respectively. FAB mass spectra were collected on a VG ZAB-SE spectrometer with a glycerin/3-nitrobenzyl alcohol matrix. Desert Analysis, Oneida Research Services, Inc., National Chemical Consulting, Inc., or Chemisar Laboratories Inc. performed the elemental analyses.

Preparation of Ph_2NNH_2. NaOH (150 mg, 3.75 mmol) was dissolved in 100 mL of water. This solution was added dropwise with stirring to 500 mg (2.27 mmol) of Ph_2NNH_2·HCl. The mixture was stirred for 1.5 h, transferred to a separatory funnel, and extracted three times with CH_2Cl_2 (3 × 2 mL). The CH_2Cl_2 solution was dried with $CaSO_4$. The dry solution was separated from the $CaSO_4$, and all volatiles were removed in vacuo. Crystallization of the resulting oily residue was achieved by dissolving the oil in a minimum amount of hexane and cooling overnight at −30 °C. The product was isolated by decanting the mother liquor and drying the pale yellow crystals in vacuo. Yield: 200 mg (48%). Mp 33−35 °C.

$[(Ph_3PAu)_3(\mu\text{-}NNPh_2)]BF_4$. Ph_2NNH_2 (9.2 mg, 0.05 mmol) was added to a stirred solution of $[(Ph_3PAu)_3(\mu\text{-}O)]BF_4$ (74 mg, 0.05 mmol) in CH_2Cl_2 (0.5 mL). The solution immediately turned bright yellow. After about 10 min, excess ether was added. The resulting yellow solid was isolated by filtration, washed with ether, and dried in vacuo. Yield: 70 mg (85%). ^{31}P NMR (101 MHz, CD_2Cl_2): δ 28.7 (s). ^{1}H NMR (250 MHz, CD_2Cl_2): δ 6.85−7.45 (m, Ph). The crystal structure of this complex has been reported.[21]

$[(LAu)_3(\mu\text{-}NNBz_2)]BF_4$. L = PPh_3. Dibenzylhydrazine (0.17 g, 2.9 mmol) was dissolved in 1 mL of CH_2Cl_2. An aliquot of this solution (0.23 mL, 0.068 mmol) was added dropwise with stirring to $[(Ph_3PAu)_3(\mu\text{-}O)]BF_4$ (0.10 g, 0.068 mmol) dissolved in 5 mL of CH_2Cl_2 at 0 °C. After 0.5 h at 0 °C, the product was precipitated with diethyl ether as a light brown solid. Yield: 94 mg (92%). ^{31}P NMR (250 MHz, CD_2Cl_2): δ 29.4 (s). ^{1}H NMR (250 MHz, CD_2Cl_2): δ 6.8−7.4 (m, 55H, Ph), 4.18 (s, 4H, CH_2Ph).

L = $P(p\text{-}MeOC_6H_4)_3$. This complex was prepared by a procedure analogous to that used for L = Ph_3P and was isolated in an 86% yield as a pale brown solid. ^{31}P NMR (101 MHz, CD_2Cl_2): δ 25.4 (s). ^{1}H NMR (250 MHz, CD_2Cl_2): 6.6−7.4 (m, 46H, Ph), 4.16 (s, 4H, CH_2-Ph), 3.73 (s, 27H, OCH_3). FAB MS: *m/z* 1857 ($[(LAu)_3(\mu\text{-}NNBz_2)]^+$), 1647 ($[(LAu)_3]^+$), 901 ($[L_2Au]^+$), 549 ($[LAu]^+$).

$[(LAu)_3(\mu\text{-}NNMe_2)]BF_4$. L = $P(o\text{-}tol)_3$. Me_2NNH_2 (5.3 μL, 0.068 mmol) was added to a stirred CH_2Cl_2 (2 mL) solution of $[(LAu)_3(\mu\text{-}O)]BF_4$ (109 mg, 0.068 mmol). The solution rapidly turned from colorless to pale yellow. After 5 min, the off-white product was precipitated with diethyl ether, recovered by filtration, washed with ether, and dried in vacuo. Yield: 102 mg (91%). ^{31}P NMR (101 MHz, CD_2Cl_2): δ 9.6 (s). ^{1}H NMR (250 MHz, CD_2Cl_2): δ 6.82−7.61 (m, 36H, Ph), 2.37 (s, 27H, tol-CH_3), 2.62 (s, 6H, NMe_2).

L = $P(p\text{-}ClC_6H_4)_3$. This complex was prepared by a procedure analogous to that used for L = $P(o\text{-tol})_3$ and was isolated in an 85% yield as a pale brown solid. ^{31}P NMR (101 MHz, CD_2Cl_2): δ 28.4 (s). ^{1}H NMR (250 MHz, CD_2Cl_2): δ 6.64−7.75 (m, 36H, Ph), 2.78 (s, 6H, N−CH3).

L = $P(p\text{-}MeOC_6H_4)_3$. This complex was prepared by a procedure analogous to that used for L = $P(o\text{-tol})_3$ and was isolated in an 88% yield as a pale brown solid. ^{31}P NMR (250 MHz, $CDCl_3$): δ 25.9 (s). ^{1}H NMR (250 MHz, $CDCl_3$): δ 6.74−7.39 (m, 36H, Ph), 2.85 (s, 6H, N−CH_3), 3.78 (s, 27H, O−CH_3).

L = $P(p\text{-}FC_6H_4)_3$. This complex was prepared by a procedure analogous to that used for L = $P(o\text{-tol})_3$ and was isolated in an 83% yield as a pale brown solid. ^{31}P NMR (250 MHz, $CDCl_3$): δ 27.5 (s). ^{1}H NMR (250 MHz, $CDCl_3$): δ 6.76−7.50 (m, 36H, Ph), 2.89 (s, 6H, N−CH_3).

L = $P(p\text{-tol})_3$. This complex was prepared by a procedure analogous to that used for L = $P(o\text{-tol})_3$ and was isolated in an 78% yield as a pale brown solid. ^{31}P NMR (250 MHz, $CDCl_3$): δ 27.9 (s). ^{1}H NMR (250 MHz, $CDCl_3$): δ 7.01−7.33 (m, 36H, Ph), 2.84 (s, 6H, N−CH_3), 2.34 (s, 27H, ring-CH_3).

L = PPh_3. This complex was prepared by a procedure analogous to that used for L = $P(o\text{-tol})_3$ and was isolated in an 92% yield as a pale brown solid. Anal. calcd (found) for $C_{56}H_{51}Au_3BF_4N_2P_3$: C, 44.17 (44.30); H, 3.38 (3.37); N, 1.84 (1.80). ^{31}P NMR (250 MHz, $CDCl_3$): δ 29.2 (s). ^{1}H NMR (250 MHz, $CDCl_3$): δ 7.25−7.48 (m, 45H, Ph), 2.82 (s, 6H, N−CH_3). FAB MS: *m/z* 1435 ($[(LAu)_3(\mu\text{-}NNMe_2)]^+$), 1377 ($[(LAu)_3]^+$), 721 ($[L_2Au]^+$), 459 ($[LAu]^+$).

L = $PEtPh_2$. This complex was prepared by a procedure analogous to that used for L = $P(o\text{-tol})_3$ and was isolated in an 85% yield as a pale brown solid. ^{31}P NMR (101 MHz, CD_2Cl_2): δ 29.8 (s). ^{1}H NMR (250 MHz, CD_2Cl_2): δ 7.97−7.02 (m, 30H, Ph), 2.84 (s, 6H, NMe_2), 2.45 (dq, J_{H-H} = 7.6 Hz, J_{H-P} = 10.4 Hz, 6H, CH_2CH_3), 1.17 (dt, J_{H-P} = 21.3 Hz, 9H, CH_2CH_3).

L = PPr^iPh_2. This complex was prepared by a procedure analogous to that used for L = $P(o\text{-tol})_3$ and was isolated in an 80% yield as a pale brown-yellow solid. ^{31}P NMR (101 MHz, CD_2Cl_2): δ 43.3 (s). ^{1}H NMR (250 MHz, CD_2Cl_2): δ 7.85−7.11 (m, 30H, Ph), 2.93 (s, 6H, NMe_2), 2.91 (dsept, J_{H-H} = 6.8 Hz, J_{H-P} = 12.6 Hz, 3H, $CH(CH_3)_2$), 1.18 (dd, J_{H-P} = 19.5 Hz, 18H, $CH(CH_3)_2$).

$[(LAu)_3(\mu\text{-}NOH)]BF_4$. L = $P(o\text{-tol})_3$. NH_2OH (5 mg, 0.2 mmol) was added to a CH_2Cl_2 (1 mL) solution of $[(LAu)_3(\mu\text{-}O)]BF_4$ (50 mg, 0.031 mmol). After 10 min, the product was precipitated with diethyl ether as a white solid. Yield: 93%. White crystals suitable for X-ray analysis were obtained from concentrated THF solutions at room temperature. ^{31}P NMR (101 MHz, CD_2Cl_2): δ 6.5 (s). ^{1}H NMR (250 MHz, CD_2Cl_2): δ 6.84−7.53 (m, 36H, Ph), 4.76 (q, J_{P-H} = 2.13 Hz, 1H, OH), 2.39 (s, 27H, CH_3). IR (mineral oil, cm^{-1}): 3437 m (ν_{OH}).

L = PPh_3. This complex was prepared by a procedure analogous to that used for L = $P(o\text{-tol})_3$. However, the complex is very unstable in solution (complete decomposition to $[(LAu)_6]^{2+}$ after 20 min at ambient temperatures) and could not be isolated in pure form. ^{31}P NMR (101 MHz, CD_2Cl_2): δ 29 (s). The ^{1}H NMR spectrum shows a quartet for the NOH group similar to that for the L = $P(o\text{-tol})_3$ derivative.

$[(AuPPh_3)_3NCl](BF_4)$. $[(Ph_3PAu)_3(\mu\text{-}O)]BF_4$ (100 mg, 0.062 mmol) was dissolved in 10 mL of CH_2Cl_2. The solution was cooled to 0 °C, and freshly prepared chloroamine (ca. 1 M in diethyl ether) was added until ^{31}P NMR spectra of the reaction mixture showed complete consumption of the oxo complex (24 ppm). The product was precipitated with diethyl ether as a white solid. Yield: 56 mg (56%). ^{31}P NMR (250 MHz, CH_2Cl_2): δ 29.1. Anal. calcd (found) for $C_{54}H_{45}Au_3BClF_4NP_3$: C, 42.8 (43.1); H, 2.97 (3.01); N, 0.92 (0.74).

$[(LAu)_6](BF_4)_2$. L = $P(p\text{-}ClC_6H_4)_3$. $[(LAu)_3(\mu\text{-}NNMe_2)]BF_4$ (55 mg, 0.03 mmol) was dissolved in THF with stirring. A deep red solution was generated in 1 h. Excess ether was added. The red-brown solid product was isolated by filtration, washed with ether, and dried in vacuo. Yield: 48.4 mg (91%). ^{31}P NMR (101 MHz, CD_2Cl_2): δ 57.6 (s). UV−vis (THF): λ_{max} (nm) 408, 295, 252. Anal. calcd (found) for $C_{108}H_{72}Au_6B_2F_8Cl_{18}N_2$: C, 36.55 (36.12); H, 2.04 (2.03).

L = PPr^iPh_2. $[(LAu)_3(\mu\text{-}NNMe_2)]BF_4$ (56.8 mg, 0.04 mmol) was dissolved in THF with stirring. A cloudy solution formed after 0.5 h. The reaction mixture was stirred for 2 days. The resulting precipitate was recovered by filtration, washed with THF, and dried in vacuo. Yield: 39.2 mg (72%). The NMR spectra are exchange-broadened at ambient temperatures (see the text). ^{31}P NMR (101 MHz, CD_2Cl_2): δ 71.1 (br s, $\nu_{1/2}$ = 2500 Hz). ^{31}P NMR (−50 °C, 202 MHz, CD_2Cl_2): δ 78.1 (s, 2P), 67.6 (s, 4P). ^{1}H NMR (500 MHz, CD_2Cl_2): δ 3.6 (br s, $\nu_{1/2}$ = 37.5 Hz), 2.91 (br s, $\nu_{1/2}$ = 31.3 Hz), 1.2 (br s, $\nu_{1/2}$ = 37.5 Hz), 1.03 (br s, $\nu_{1/2}$ = 37.5 Hz). UV−vis (CH_2Cl_2): ν_{max} (nm) 474, 446, 310, 280, 268, 234. A similar procedure gives the known PPh_3 (96%) and $P(p\text{-tol})_3$ derivatives.[11]

$[(Au_{11}(PPh_2Me)_{10}](BF_4)_3$. Me_2NNH_2 (3 mg, 0.05 mmol) was added to a white suspension of $[(Ph_2MePAu)_3(\mu\text{-}O)]BF_4$ (66.8 mg, 0.05 mmol) in THF (2 mL) with stirring. A homogeneous red solution rapidly formed. After the solution was stirred for 2 h, a red precipitate along with a deep red solution had formed. All volatiles were removed in vacuo, and the red residue was dissolved in 2 mL of CH_2Cl_2. The CH_2Cl_2 solution was filtered through Celite, and excess ether was added. The resulting red solid was isolated by filtration, washed with ether, and dried in vacuo. Yield: 48.7 mg (88.0%). A similar procedure gives

the PMe_2Ph derivative. Spectroscopic data (NMR and UV−vis) for both derivatives agree with literature values.[11]

$[(Ph_3PAu)_3(\mu\text{-}NNEtMe_2)](OTf)(BF_4)$. Ethyl triflate (0.05 mmol, 8.0 mL) was added to a CH_2Cl_2 (2 mL) solution of $[(Ph_3PAu)_3(\mu\text{-}NNMe_2)]BF_4$ (0.033 mmol, 50 mg). After 2 min, the yellow solid product was precipitated with diethyl ether. Yield: 45 mg (88%). ^{31}P NMR (250 MHz, CD_2Cl_2): δ 29.6 (s). ^1H NMR (250 MHz, CD_2Cl_2): δ 7.25−7.53 (m, 45H, Ph), 4.11 (q, $J_{H-H} = 7.1$ Hz, 2H, NCH_2CH_3), 1.80 (t, 3H, NCH_2CH_3), 3.66 (s, 6H, NMe_2).

$[(Ph_3PAu)_3(\mu\text{-}NNRMe_2)](OTf)_2$. R = Et. This complex was prepared in a manner similar to that of $[(Ph_3PAu)_3(\mu\text{-}NNEtMe_2)](OTf)(BF_4)$ above by using $[(Ph_3PAu)_3(\mu\text{-}NNMe_2)]OTf$ in place of $[(Ph_3PAu)_3(\mu\text{-}NNMe_2)]BF_4$. Yield: 95%. NMR spectroscopic data were identical to those of the mixed salt above. Anal. calcd (found) for $C_{60}H_{56}Au_3F_6N_2O_6P_3S_2$: C, 40.9 (41.6); H, 3.2 (3.2); N, 1.6 (1.6). Crystals for the X-ray diffraction study were grown from a THF solution layered with Et_2O (−20 °C).

R = Me. This complex was prepared in a manner similar to that of $[(Ph_3PAu)_3(\mu\text{-}NNEtMe_2)](OTf)(BF_4)$ above by using $[(Ph_3PAu)_3(\mu\text{-}NNMe_2)]OTf$ in place of $[(Ph_3PAu)_3(\mu\text{-}NNMe_2)]BF_4$ and methyl triflate in place of ethyl triflate. Yield: 95%. ^{31}P NMR (250 MHz, CD_2Cl_2): δ 29.7 (s). ^1H NMR (250 MHz, $CDCl_3$): δ 7.26−7.50 (m, 45H, Ph), 3.84 (s, 9H, NMe_2).

Kinetic Measurements. Method 1 (L = PPh_3 Only). $[(Ph_3PAu)_3(\mu\text{-}NNMe_2)]BF_4$ (5.8 mg) was dissolved in 0.70 mL of CH_2Cl_2. The reaction was followed by monitoring the decrease in integrated ^{31}P NMR intensity of the resonance of the starting complex $[(AuPPh_3)_3(\mu\text{-}NNMe_2)]BF_4$ with respect to the increase in intensity of the resonance of the product $[(AuPPh_3)_6](BF_4)_2$. ^{31}P NMR spectra were recorded every 6 min for 1 h. The temperature was maintained at 298 K.

Method 2. Solid $[(LAu)_3(\mu\text{-}NNMe_2)]BF_4$ (15 mg) was mixed with $[PMe_2Ph_2]BF_4$ (5 mg) in a 5 mm NMR tube. CH_2Cl_2 (0.50 mL) was added, and the sample was transferred to the NMR probe set at the desired temperature. The sample was scanned every 2 min for a total time of about 40 min, depending on the half-life of the compound. Early time points (1−5 min), where the sample was thermally equilibrating with the probe, were discarded. The signal from $PMe_2Ph_2^+$ was used as an internal integration standard for the reacting hydrazido complex. This method gave results identical to those of method 1 (L = PPh_3), indicating that the internal standard does not alter the decomposition of the complex.

Acknowledgment. We thank the Division of Chemical Sciences, Office of Basic Energy Sciences, Office of Energy Research, U.S. Department of Energy (Grant DF-FG02-88ER13880) for support of this work. Grants from the National Science Foundation provided a portion of the funds for the purchase of X-ray (CHE-9011804) and NMR (PCM-8115599 and CHE 89-08304) equipment. The University of Missouri Research Council Board provided funding for upgrading the data acquisition system of the mass spectrometer. We thank Amanda Crawford for preliminary work on the decomposition kinetics, Dr. Visalakshi Ramamoorthy for early synthetic work, and Dr. D. Zagorevski for the mass spectral measurements.

Supporting Information Available: Kinetic and Arrhenius plots and tables and two X-ray crystallographic files, in CIF format. This material is available free of charge via the Internet at http://pubs.acs.org.

IC990586U